ZnCdSe Quantum Structures - Growth, Optical Properties and Applications

Martin Strassburg[1], O. Schulz[1], Matthias Strassburg[1], U.W. Pohl[1], R. Heitz[1], A. Hoffmann[1], D. Bimberg[1], M. Klude[2], D. Hommel[2], K. Lischka[3], and D. Schikora[3]

[1] Technische Universität Berlin, Institut für Festkörperphysik, 10623 Berlin, Germany
[2] Universität Bremen, Institut für Festkörperphysik, 28359 Bremen, Germany
[3] Universität Paderborn, Fachbereich 6 - Physik, 33098 Paderborn, Germany

Abstract. ZnCdSe quantum structures are investigasted for the effect of exciton localisation on the potential for opto-electronic applications. The investigation on ZnCdSe quantum dots as the active material in a laser diode and their temperature dependece show a transition from 0D-like to 2D-like characteristics limiting their capabiblity for devices. Furthermore, optimisation of electrical contacts due to a post-growth increase of the p-type doping level and efficient index guiding allowing a substantial decrease of losses improving the lifetime of laser diodes more than 20 times.

Semiconductor quantum structures have been widely studied for the possibility to engineer electronic and optical properties being essential also for optimising opto-electronic devices. The fabrication of semiconductor (SC) light emitters and laser diodes (LDs) gives access to a large field of applications, e.g. laser TV and polymer optical fibre communication technology. Mixing of suitable discrete laser transitions will allow to cover the whole color spectrum. Thus, for the implementation of displays, projector devices and laser televison, blue, green and red emitting LDs are necessary. However, until now, the development of such devices is prevented by the lack of commercial green-emitting LDs with sufficient lifetime. Based on GaN and GaAs blue and red emitting LDs are realised, respectively. Especially, the introduction of zero-dimensional centres for light generation enabled the commercial breakthrough of UV and blue LDs [1] and lead to significant improvements in GaAs-based LDs [2]. The investigations of proper materials for the green-emitting LDs were focused on ZnCdSe and InGaN due to their optically properties (e.g., bandgap energy, oscillator strength,). Although electrically pumped lasing was demonstrated in ZnSe-based quantum structures more than ten years ago [3], a breakthrough for green LDs was not achieved, yet.

The aim of this paper is to present and evaluate approaches and results leading to a significantly enhanced lifetime of ZnSe-based LDs. As it was shown by Sony Corp., which still holds the lifetime record of about 500 h for ZnSe LDs using a ZnCdSe QW as active region [4], the lifetime is limited by heat induced defect generation. In II-VI LDs, the heat production is

much larger than in III-V LDs, because of the large series resistance, which originates from the non-ohmic contacts [5]. This heat accelerates the formation of so-called dark-line defects which cause a degradation of the active area and, hence of the whole device [6]. Thus, novel approaches to increase the lifetime of ZnSe-based LDs have to reduce the heat generation. Therefore, the whole device has to be improved to reduce the electrical and optical losses. Introducing quantum dot (QD) ensembles for the active region, novel contacts, and current- and wave-guiding, we will present improvements on several areas of ZnCdSe LDs. The impact on heat reduction is discussed and significantly lifetime extension is presented.

1 Quantum Dots in the Active Region: 0D Localisation and Mobility of Excitons

The active region of a ZnSe-based LD usually consists of single or multi-layered stacks of ZnCdSe QWs, where non-radiative processes lead to heat generation. The in-plane mobility allow charge carriers to migrate to defects, where their non-radiative recombination contributes to the heating of the LD.

In recent years, the role of QDs as active region for ZnSe-based LDs has increased tremendously driven by enhanced linear and nonlinear optical properties compared to systems of higher dimensionality, and of course, by improving growth techniques. The introduction of QDs as active regions is advantageously, as it was demonstrated e.g., for red- and near-infrared-emitting LDs [2]. The extraordinary properties of QDs (e.g. discrete electronic levels, thermal stability of states, high (excitonic) gain, low density of states) enable the realisation of new principles in light emitting devices. It is known that the 3D confinement of carriers and excitons allows zero-phonon lasing [7] and exciton waveguiding [8], which provides for efficient optical confinement in a narrow spectral range. The enhanced wave-guiding could decrease optical losses. Therefore, one might expect a lowering of the lasing threshold and consequently a reduction of heat generation in such devices. However, ZnCdSe LDs with QDs in the active region, as shortly described above, have not been realised, yet. A possible explaination might be the insufficient localisation of excitons/carriers in such QD structures. Even, for structures showing optically pumped 0D lasing up to RT, insufficient p-conductivity of the cladding layers prevents succesful LD operation [9].

Why does 3D confinement of carriers/excitons not persist at RT in ZnCdSe QD structures? Therefore, the selforganised growth of II-VI QDs is evaluated. Due to the lattice mismatch between CdSe and ZnSe (Δ a/a $>$ 7 %), which is very similar to that of the InAs/GaAs system, and the respective band discontinuities a growth of type I QD heterostructures is enabled by selforganised island formation. Generally, high-quality QD structures have been demonstrated by numbers of research groups and

commercial companies. Dense arrays of islands (up to several 10^{10} cm^{-2}) with island sizes ranging from about 10 nm to above 100 nm are grown by MBE in the Stranski-Krastanov mode [10–12].

Using appropriate growth conditions even higher island densities and smaller island sizes are realised by MBE and MOCVD techniques due to an inhomogeneous distribution of Cd in the deposited QW [13,14]. These inhomogeneities are generated by sub-monolayer growth and/or segregation of Cd during the capping procedure [15]. Such islands formed by Cd-rich

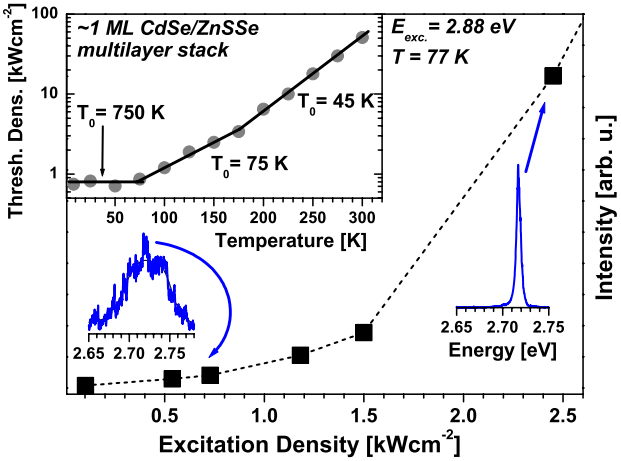

Fig. 1. Intensity of an optically pumped laser structure with CdSe/ZnSSe multilayered QDs in the active region. The spectra were recorded at the excitation densities marked by arrows. The inset shows the threshold density as a function of temperature. The decrease of characteristic temperatures T_0 with increasing temperature reflects the 0D- to 2D-like emission characteristics at low and elevated temperatures, respectively.

regions in a ZnCdSe alloy QW have densities up to 10^{12} cm^{-2}. Obviously, the ZnCdSe system allowes for structures with dense arrays of nm-scaled islands providing 3D confinement for carriers and excitons. QD-like behaviour of such structures was confirmed e.g. by photo- and cathodoluminescence investigations performed at lower temperatures.

0D lasing mechanisms in II-VI QD structures have been extensively studied, especially at low temperatures. For an example, excitonic and biexcitonic gain and zero-phonon lasing are reported. In this way, and especially at low temperatures it was confirmed that ZnCdSe QDs meet theoretical predictions for novel laser structures. The large potential offered by ZnCdSe QDs for LDs is illustrated by an example, shown in Fig. 1. For a MOCVD-grown multilayered stack of ZnCdSe QDs in a ZnSSe matrix a low threshold density in optically pumped QD laser is realised. A lasing threshold density well below

1 kWcm^{-2} is observed, which is about five times less than in comparable QW structures [16]. The low threshold density is attributed to 0D excitons. This is confirmed by a high characteristic temperature T_0. In ideal QDs an infinite T_0 is expected, whereas in QW lasers T_0 is well below 100 K. The observed decrease in T_0 above T = 100 K is attributed to the delocalisation of excitons and carriers from the QDs. Thermal activation increases the exciton mobility and enables the transition in higher states, i.e. the QW, resulting in 2D-like excitons/carriers.

These experiments show, that localisation energy of excitons/carriers up to room temperature (RT) is problematically in ZnCdSe QD structures. Hence, it is essential to identify the origin and mechanisms of exciton/carrier mobility and, possible identifying means to preserve 0D behaviour up to RT.

Such investigations on the localisation and mobility of 0D and 2D excitons are presented, now. Localisation at interface roughness and fluctuations lead to 0D-like behaviour in QW structures. The influence of the respective confinement potentials on excitons and carriers has been investigated for CdSe- and ZnSe based QW structures for more than twenty years. However, the role of the exciton mobility, even in the case of quasi-3D confinement in QDs, i.e. for the localisation and delocalisation in 0D-like ZnSe- and CdSe-based structures, was met with increasing interest in recent years [17,18]. Though different theoretical approaches were introduced to explain such experiments, the most striking result was the persistent mobility of excitons and carriers in the presence of 0D localisation sites and, furthermore, even at low temperatures for which an ideal QD behaviour was expected. The mobility is caused by exciton or carrier transfer processes between QDs. Depending on the localisation energy of the exciton, such transfer might be more probable than radiative recombination. Such a behaviour can be described by a mobility edge representing the energy above which transfer and 2D-like behaviour occur even in QD structures. A trivial example for a mobility edge is given by the 2D wetting layer state, which is the first common electronic state for QDs grown in SK mode. In real QD structures, the mobility edge is observed well below the wetting layer energy and is attributed to the presence of a large number of energy states provided by a high-density of QDs.

Therefore, a redistribution of excitons is enabled among the QD ensemble from 0D sites with higher transition energies to 0D sites with smaller transition energies. At low temperatures the transfer is assigned to tunnel processes and, hence, is observed particularly in high-density QD ensembles. With increasing temperature, the difference between QD groundstate and barrier energies is decreased by thermal activation of excitons/carriers. Additionally, phonon-assisted escape becomes more probably and supports the lateral mobility of excitons/carriers.

Such transfer processes lead to a characteristic variation of PL decay time as a function of the detection energy. The decay time increases with the detection energy and shows saturation for energies given by QDs with

large localisation energy for excitons. This behaviour originates from transfer processes being faster than the radiative decay of 0D excitons in the ZnCdSe system. Time-resolved investigations allow the determination of the radiative lifetime and the mobility edge in QD structures [18], as shown for an inhomogeneous broadened ZnCdSe-QD ensemble and a QW in Fig. 2. It is known

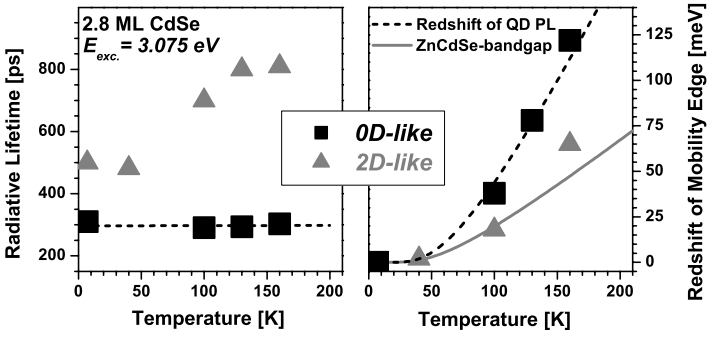

Fig. 2. Radiative lifetime and redshift of the mobility edge for (0D-like) quantum dot and (2D-like) quantum well structures as a function of temperature.

that the radiative transition rate is proportional to the overlap of the carrier wavefunction. For strongly localised excitons the overlap remains constant. Hence, the radiative lifetime is expected to be independent of temperature for QD transitions. This is confirmed for the investigated QD structure. The QW reference sample shows an pronounced increase of radiative lifetime with temperature, when the thermal energy overcomes the localisation energy of excitons in QW inhomogeneities (e.g., islands formed by Cd fluctuations or thickness fluctuations of the QW). The temperature dependence of the mobility edge (see Fig. 2) reveals that only a significantly reduced amount of QDs provides 0D-like localisation up to elevated temperatures. Although the PL is still generated in 0D centres, what is confirmed by a parallel redshift of the PL maximum and the mobility edge, this pronounced redshift illustrates that with rising temperature more and more QDs allow the transfer to lower energy states. In comparison to that, in QW structures the mobility edge follows the temperature dependence of the bandgap [19].

Finally, the transfer of excitons/carriers between QDs results in a 2D-like behaviour. 0D-like lasing and the implementation of an excitonic waveguiding are not yet achieved at RT. Therefore, until now, the improvement of ZnCdSe-based LDs using QDs in the active region is by far not as high as expected. A significant reduction of losses and, thus, a lowering of parasitic heat generation is not demonstrated. Nevertheless, mechanisms determining exciton/carrier mobility are identified. The suppression of high-density energy states of QDs formed by Cd fluctuations is proposed and examined to reduce carrier mobility [20–23], and thus provide thermally more stable ex-

citon/carrier localisation. The implementation of such QD structures might provide the expected properties of the active region, but they are still under investigation.

2 Optimisation of p-contacts and p-claddings

While the improvement of the active region still suffers from incompatibility to RT operation, the optimisation of the entire laser structure becomes indispensable. ZnSe-based lasers consist of a separate confinement heterostructure (SCH). The structure is generally grown on n-type GaAs-substrate. The n-side of the laser comprise ZnSe and ZnSSe buffer layers, a ZnMgSSe cladding layer and a ZnSSe waveguide. Free electron concentrations range from $2 \cdot 10^{18}\ cm^{-3}$ for binary to $4 \cdot 17^{17}\ cm^{-3}$ for quaternary compounds. The active region is a ZnCdSSe QW, which is followed by a p-ZnSSe waveguide, a p-ZnMgSSe cladding layer, a p-ZnSSe spacer and the p-contact composed of ZnSe, ZnSeTe and ZnTe. Free hole concentrations are between $1 \cdot 10^{18}\ cm^{-3}$ for binary and $6 \cdot 10^{16}\ cm^{-3}$ for quaternary layers. Details of the growth and design of the laser structures can be found elsewhere [24].

Present issues of LD improvement mainly focus on the poor electrical characteristics. While the n-type doping levels of the device are sufficiently high, the p-type doping, in particular of the ZnMgSSe cladding, is still a limiting factor in the performance of a laser diode. Furthermore, there exist no ohmic contacts to p-ZnSe due to its large bandgap energy and electron affinity that sum up to 6.7 eV thus exceeding the workfunction of metals [25]. Holes can hence only be injected by tunneling through the Schottky barrier. A high tunneling rate requires a narrow barrier width. Since the p-type doping of ZnSe is limited to about $2 \cdot 10^{18}\ cm^{-3}$ due to compensation effects [26], the achievement of higher acceptor concentration during MBE growth turned out to be not feasable. Thus, a strongly strained ZnTe/ZnSe-MQW structure was introduced [27,28]. To avoid strain induced defects and hence stronger compensation of the nitrogen acceptor in p-ZnSe, it is important to keep the thickness of the ZnTe-toplayer below 4 nm [29].

Finally, the solution can be either in-diffusion of additional acceptors or a reduction of the compensation level of the nitrogen dopant, which was used for p-type doping during MBE growth. In-diffused additional acceptors must have less compensation than the built-in nitrogen acceptor. Since both, Li and N form shallow acceptor states in II-VI compounds, Li_3N is considered as a promising candidate for co-doping. It was previously shown that ZnSe can be doped p-type in MOCVD using Li_3N [30]. Nevertheless, the applied growth temperature of 450 C is too high for laser diodes due to the enhanced diffusion of group II elements at temperatures above 400 C [31]. In this contribution, the characteristics of structures with post growth applied Li_3N are studied. Li_3N, Pd and Au are evaporated to form the p-electrode for ZnSe-based devices [32]. The diffusion of Li_3N is caused by the heat during metallisation

and a subsequent rapid thermal annealing at 225 C. In-diffusion of Li and N were proven by secondary ion mass spectroscopy (Fig. 3(a)). A simultaneous increase of the Li and N concentrations in the p-ZnMgSSe cladding of a LD is observed. The SIMS depth profiles reveal that Li and N diffuse in

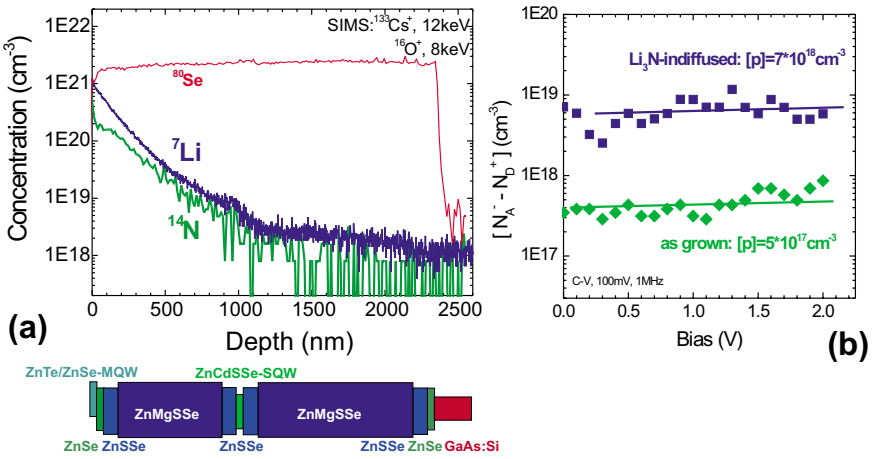

Fig. 3. Depth profile of a ZnCdSSe laser diode, demonstrating the increase of Li and N concentration due to indiffusion after deposition of a Li_3N/Pd/Au electrode. The sample structure shown below corresponds to the same depth scaling and indicates the respective bandgaps (a). Enhancement of the free hole concentration of a p-type ZnSe:N layer with a p-ZnTe/ZnSe MQW (b).

parallel into the p-side of the laser structure (except for a thin layer near the p-contact). This is a clear indication of complex formation. The ratio of Li and N lies between 2 and 3 in the entire p-side. Therefore we assume that Li and N are commonly diffusing into the lattice as a Li_xN-complex. The concentration of nitrogen in the p-ZnMgSSe cladding is enhanced to values between $7 \cdot 10^{18}$ cm^{-3} and $9 \cdot 10^{19}$ cm^{-3}. A further hint of Li_xN-complex formation is the pronounced improvement of the laser characteristics. Compared to lasers with standard Pd/Au electrodes, a significant reduction of the threshold current density from 250 A/cm^2 to below 50 A/cm^2 and a decrease of the operating voltage by 20 % down to 5.5 V accompanied by an increase of the differential quantum efficiency of 50 % lead to a lifetime extension by more than a factor of 20 with a total cw-lifetime of 9.5 h [33,34]. These improvements can be explained with an enhanced free hole concentration, leading to a current guiding below the stripe contact and hence an reduced threshold current density and a reduced Schottky barrier width lowering the operation voltage [35]. If Li and N would act as single acceptors, such large concentration of Li and N show strong compensation effects [36,37]. Thus, a

dramatic deterioration of the laser performance would have been expected. Since the benefit of the Li_3N in-diffusion is so obvious, an enhancement of the free hole concentration is assumed due to Li_xN acting as an acceptor complex.

The increase of the p-type doping level is verified independently by C-V profiling. Therefore, the free hole concentration of an as grown test structure consisting of a p-ZnSe-layer and a standard ZnTe/ZnSe-MQW contact structure is compared to a similar structure with an additional in-diffused Li_3N layer. To contact the sample surface, the Li_3N/Pd/Au electrode must be removed by reactive ion etching after its evaporating and subsequent annealing. For C-V profiling, mercury is used to create Schottky contacts on the sample surface. The formation of the Schottky contact was confirmed by I-V profiling. While the free hole concentration of the as grown structure is $5 \cdot 10^{17}\ cm^{-3}$, it is increased by more than one order of magnitude after Li_3N in-diffusion to $7 \cdot 10^{18}\ cm^{-3}$ (Fig. 3(b)). This demonstrates that the in-diffused Li_3N-complex acts as an acceptor.

3 Optical Confinement

Using the potential of lateral waveguiding in ZnSe-based LDs, losses and thus heat generation can be further reduced. In gain guided LD structures guiding of the lightwave is achieved in vertical direction by the waveguide layers which embed the active QW. Lateral guiding arises from the stripe contact geometry for providing a laterally structured carrier injection (Fig. 4(a)). To improve the performance of ZnSe-based LDs an additional lateral index guiding might be introduced to support the gain guiding (Fig. 4(b)). Such an

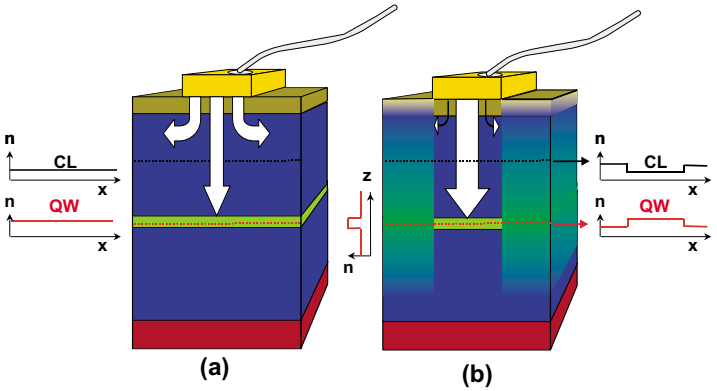

Fig. 4. Comparison of gain (a) and index guided laser structure created by ion implantation (b). The insets show the refractive index in the active region and the cladding. For details see discussion in the text.

optimised guiding of the lightwave can be obtained via laterally structured ion implantation. Ions with an appropriate energy to generate a maximal amount of vacancies near the active region are used, because the diffusion of group II components is enhanced by vacancies [31]. Hence the interfaces between the layers will be intermixed in irradiated regions. Details of the used implantation technique are described elsewere [38]. The diffusion of the Cd into the waveguide lowers the refractive index of the active region in the implanted and intermixed parts of the structure. Thereby, a small step of the refractive index is generated in the lateral direction. Simultaneously, the intermixing increases the refractive index of the waveguide and cladding in the implanted and intermixed regions of the structure. A small, negative step of the refractive index and thus an anti-waveguide is generated below and above the plane of the active region (Fig. 4(b)). The stripewidth of the laser is limited by the resist which forms the implantation mask and the intermixing of the stripe edges during ion implantation. Thus, a total stripewidth of < 5 μm can be achieved. Such small stripewidth is necessary for fundamental optical mode (TEM_{00}) emission. In addition to the refractive index variation, a blocking of the current spread occures due to defects in the intermixed regions (see white arrows in Fig. 4). These defects generate highly resistive material beneath the stripe. Such lasers are fully index guided. Since both, the light wave and the current are guided in such structures, losses will be reduced. Therefore, low threshold current densities and increased differential quantum efficiencies are expected for fully index guided lasers. The obtained results prove the applicability of ion implantation for ZnSe-based LDs. The current density is reduced by a factor of three down to 96 A/cm^2 and the differential quantum efficiency is more than doubled [39,40]. Due to the reduced optical losses, higher modes are suppressed. Finally, the lifetime of LDs is extended by a factor of up to five.

4 Conclusions

We have presented that the characteristics of ZnCdSe QDs as material for the optically activ region are superior to that of corresponding QWs. Due to thermally activated transfer processes and week localisation these advantages vanish at RT. Since the mobility edge shows a strong redshift, even deep localising QDs behave 2D-like. Therefore, the increase of thermal stability is the main issue for the future development of ZnCdSe QDs. Using post growth enhancement of the p-type doping and lateral index guiding, electrical and optical losses in ZnCdSe QW lasers are reduced. Hence, remarkable low threshold current densities below 50 A/cm^2 are obtained. All these improvements lead to an increase of the cw-lifetime of a factor of more than 20 demonstrating the optimisation potential of ZnCdSe QW lasers.

5 Acknowledgement

The authors highly appreciate expert assistance of J. Krauser for ion implantation and J. Christen and Zh.I. Alferov for fruitful discussion.

References

1. S. Nakamura, Science **281**, 956 (1998).
2. for a review see D. Bimberg, M. Grundmann and N.N. Ledentsov, *Quantum Dot Heterostructures*, Wiley, (1999).
3. M.A. Haase, J. Qiu, J.M. DePuydt, and H. Cheng, Appl. Phys. Lett. **59**, 2992 (1991).
4. E. Kato, H. Noguchi, M. Nagai, H. Okuyama, S. Kijima, and A. Ishibashi, Electr. Lett. **34**, 282 (1998).
5. K. Kondo, H. Okuyama, and A. Ishibashi, Appl. Phys. Lett. **64**, 3434 (1994).
6. G.M. Haugen, S. Guha, H. Cheng, J.M. DePuydt, M.A. Haase, G.E. Hfler, J. Qiu, and B.J. Wu, Appl. Phys. Lett. **66**, 358 (1994).
7. N.N. Ledentsov, I.L. Krestnikov, M.V. Maksimov, S.V. Ivanov, S.V. Sorokin, P.S. Kop'ev, Zh.I. Alferov, D. Bimberg, and S.M. Sotomayor Torres, Appl. Phys. Lett. **69**, 1343 (1996).
8. Zh.I. Alferov, S.V. Ivanov, P.S. Kop'ev, A.V. Lebedev, N.N. Ledentsov, M.V. Maximov, I.V. Sedova, T.V. Shubina, and A.A. Toropov, Superl. and Microstr. **15**, 65 (1994).
9. A.V. Sakharov, S.V. Ivanov, S.V. Sorokin, I.L. Krestnikov, B.V. Volovik, N.N. Ledentsov, P.S. Kop'ev, Techn. Phys. Lett. **23**, 305 (1997).
10. M. Rabe, M. Lowisch, and F. Henneberger, J. Cryst.Growth **184/185**, 248 (1998).
11. D. Schikora, S. Schwedhelm, D.J. As, K. Lischka, D. Litvinov, A. Rosenauer, D. Gerthsen, M. Strassburg, A. Hoffmann, and D. Bimberg, Appl. Phys. Lett. **76**, 418 (2000).
12. K. Maehashi, N. Yasui, Y. Murase, T. Ota, T. Noma, and H. Nakashima, J. Electr. Mat. **29**, 542 (2000).
13. S. V. Ivanov, A. A. Toropov, S. V. Sorokin, T. V. Shubina, I. V. Sedova, A. A. Sitnikova, P. S. Kopev, Zh. I. Alferov H.-J. Lugauer, G. Reuscher, M. Keim, F. Fischer, A. Waag, and G. Landwehr, Appl. Phys. Lett. **74**, 498 (1999).
14. R. Engelhardt, U.W. Pohl, D. Bimberg, D. Litvinov, A. Rosenauer, and D. Gerthsen, J. Appl. Phys. **86**, 5578 (1999).
15. N. Peranio, A. Rosenauer, D. Gerthsen, S. V. Sorokin, I. V. Sedova, and S. V. Ivanov, Phys. Rev. B **61**, 16015 (2000).
16. F. Kreller, J. Puls, and F. Henneberger, Appl. Phys. Lett. **69**, 2406 (1996).
17. S. Yamaguchi, H. Kurusu, Y. Kawakami, Sz. Fujita, and Sg. Fujita, Phys. Rev. B **61**, 10303 (2000). see also: A. Klochikhin, A. Reznetsky, S. Permogorov, T. Breitkopf, M. Grn, M. Hetterich, C. Klingshirn, V. Lyssenko, W. Langbein, and J.M. Hvam, Phys. Rev. B **59**, 12947 (1999); L.E. Golub, S.V. Ivanov, E.L. Ivchenko, T.V. Shubina, A.A. Toropov, J.P. Bergman, G.R. Pozina, B. Monemar, and M. Wilander, Phys. Stat. Sol. (b) **205**, 203 (1998).
18. M. Strassburg, M. Dworzak, H. Born, R. Heitz, A. Hoffmann, M. Bartels, K. Lischka, D. Schikora, and J. Christen, Appl. Phys. Lett. **80**, 473 (2002).

19. K.P. O'Donnell, P.G. Middleton, in *Properties of Wide Bandgap II-VI-Semiconductors*, ed. R. Bhargava, INSPEC, emis Datareview series No. 17, 33 (1997).
20. M. Strassburg, M. Dworzak, A. Hoffmann, R. Heitz, U.W. Pohl, D. Bimberg, D. Litvinov, A. Rosenauer, D. Gerthsen, I. Kudryashov, K. Lischka, and D. Schikora, Phys. Stat. Sol. (a) **180**, 281 (2000).
21. E. Kurtz, M. Schmidt, M. Baldauf, S. Wachter, M. Grn, H. Kalt, C. Klingshirn, D. Litvinov, A. Rosenauer, and D. Gerthsen, Appl. Phys. Lett. **79**, 1118 (2001).
22. M. Strassburg, J. Christen, M. Dworzak, R. Heitz, A. Hoffmann, M. Bartels, K. Lischka, and D. Schikora, Phys. Stat. Sol. (b) **229**, 529 (2002).
23. T. Passow, K. Leonardi, H. Henke, D. Hommel, J.Seufert, G. Bacher, and A. Forchel, Phys. Stat. Sol. (b) **229**, 497 (2002).
24. M. Behringer, H. Wenisch, M. Fehrer, V. Grossmann, A. Isemann, M. Klude, H. Heinke, K. Ohkawa, and D. Hommel, Adv. Solid State Phys. **47**, 47 (1997).
25. Y. Koide, T. Kawakami, N. Teraguchi, Y. Tomomura, A. Suzuki, and M. Murakami, J. Appl. Phys. **82**, 2393 (1997).
26. P.M. Mensz, S. Herko, K.W. Haberern, J. Gaines, and C. Ponzoni, Appl. Phys. Lett. **63**, 2800 (1993).
27. Y. Fan, J. Han, L. He, J. Saraie, R.L. Gunshor, M. Hagerott, H. Jeon, A.V. Nurmikko, G.C. Hua, and N. Otsuka, Appl. Phys. Lett. **61**, 3160 (1992).
28. F. Hiei, M. Ikeda, M. Ozawa, T. Miyajima, and A. Ishibashi, and K. Akimoto, Electr. Lett. **29**, 878 (1993).
29. S. Tomiya, S. Kijima, H. Okuyama, H. Tsukamoto and T. Hino, S. Taniguchi, H. Noguchi, E. Kato, and A. Ishibashi, J. App. Phys. **86**, 3616 (1999).
30. T. Yasuda, I. Mitsuishi, and H. Kukimoto, Appl. Phys. Lett. **52**, 57 (1988).
31. M. Strassburg, M. Kuttler, U.W. Pohl, and D. Bimberg, Thin Solid Films **336**, 208 (1998).
32. M. Strassburg, O. Schulz, U.W. Pohl, and D. Bimberg, German Patent Nr. 19955280 (1999).
33. M. Strassburg, O. Schulz, U.W. Pohl, D. Bimberg, M. Klude, and D. Hommel, Electr. Lett. **36**, 878 (2000).
34. M. Strassburg, O. Schulz, U.W. Pohl, D. Bimberg, S. Itoh, K. Nakano, A. Ishibashi, M. Klude, and D. Hommel, IEEE J. Select. Top. Quant. Electr. **7**, 371 (2001).
35. B. Mroziewicz, M. Bugajski, and W. Nakwaski: *Physics of Semiconductor Lasers*, North Holland, (1991).
36. R. Heitz, B. Lummer, V. Kutzer, D. Wiesmann, A. Hoffmann, I. Broser, E. Kurtz, S. Einfeldt and J. Nrnberger, B. Jobst, D. Hommel, and G. Landwehr, Mat. Science Forum **182-184**, 259 (1995).
37. U.W. Pohl, G.H. Kudlek, A. Klimakov, and A. Hoffmann, J. Cryst. Growth **138**, 385 (1994).
38. O. Schulz, M. Strassburg, U.W. Pohl, D. Bimberg, S. Itoh, K. Nakano, A. Ishibashi, M. Klude, and D. Hommel, Phys. Stat. Sol. **180**, 213 (2000).
39. M. Strassburg, O. Schulz, U.W. Pohl, D. Bimberg, S. Itoh, K. Nakano, and A. Ishibashi, Electr. Lett. **36**, 44 (2000).
40. M. Strassburg, O. Schulz, U.W. Pohl, D. Bimberg, M. Klude, and D. Hommel, J. Cryst. Growth **214/215**, 1054 (2000).